BRAIN CONNECTIVITY
Volume 11, Number 10, 2021

DOI: 10.1089/brain.2020.0748

Abnormal Dynamic Functional Network Connectivity Estimated from Default Mode Network Predicts Symptom Severity in Major Depressive Disorder

Mohammad S.E. Sendi,[1–3,i,*] Elaheh Zendehrouh,[4,*] Jing Sui,[3,5–7] Zening Fu,[3] Dongmei Zhi,[3,5,6] Luxian Lv,[8,9] Xiaohong Ma,[10,11] Qing Ke,[12] Xianbin Li,[13] Chuanyue Wang,[13] Christopher C. Abbott,[14] Jessica A. Turner,[3,15,16] Robyn L. Miller,[3,4] and Vince D. Calhoun[1–4,15,16]

Abstract

Background: Major depressive disorder (MDD) is a severe mental illness marked by a continuous sense of sadness and a loss of interest. The default mode network (DMN) is a group of brain areas that are more active during rest and deactivate when engaged in task-oriented activities. The DMN of MDD has been found to have aberrant static functional network connectivity (FNC) in recent studies. In this work, we extend previous findings by evaluating dynamic functional network connectivity (dFNC) within the DMN subnodes in MDD.
Methods: We analyzed resting-state functional magnetic resonance imaging data of 262 patients with MDD and 277 healthy controls (HCs). We estimated dFNCs for seven subnodes of the DMN, including the anterior cingulate cortex (ACC), posterior cingulate cortex (PCC), and precuneus (PCu), using a sliding window approach, and then clustered the dFNCs into five brain states. Classification of MDD and HC subjects based on state-specific FC was performed using a logistic regression classifier. Transition probabilities between dFNC states were used to identify relationships between symptom severity and dFNC data in MDD patients.
Results: By comparing state-specific FNC between HC and MDD, a disrupted connectivity pattern was observed within the DMN. In more detail, we found that the connectivity of ACC is stronger, and the connectivity between PCu and PCC is weaker in individuals with MDD than in those of HC subjects. In addition, MDD showed a higher probability of transitioning from a state with weaker ACC connectivity to a state with stronger ACC connectivity, and this abnormality is associated with symptom severity. This is the first research to look at the dFC of the DMN in MDD with a large sample size. It provides novel evidence of abnormal time-varying DMN configuration in MDD and offers links to symptom severity in MDD subjects.

[1]Wallace H. Coulter Department of Biomedical Engineering, Georgia Institute of Technology and Emory University, Atlanta, Georgia, USA.
[2]Department of Electrical and Computer Engineering, Georgia Institute of Technology, Atlanta, Georgia, USA.
[3]Tri-institutional Center for Translational Research in Neuroimaging and Data Science: Georgia State University, Georgia Institute of Technology, Emory University, Atlanta, Georgia, USA.
[4]Department of Computer Science, Georgia State University, Atlanta, Georgia, USA.
[5]Brainnetome Center and National Laboratory of Pattern Recognition, Institute of Automation, Chinese Academy of Sciences, Beijing, China.
[6]School of Future Technologies, University of Chinese Academy of Sciences, Beijing, China.
[7]State Key Laboratory of Cognitive Neuroscience and Learning, Beijing Normal University, Beijing, China.
[8]Department of Psychiatry, Henan Mental Hospital, The Second Affiliated Hospital of Xinxiang Medical University, Xinxiang, China.
[9]Henan Key Laboratory of Biological Psychiatry, Xinxiang Medical University, Xinxiang, China.
[10]Psychiatric Laboratory and Mental Health Center, The State Key Laboratory of Biotherapy, West China Hospital of Sichuan University, Chengdu, China.
[11]Huaxi Brain Research Center, West China Hospital of Sichuan University, Chengdu, China.
[12]Department of Neurology, The First Affiliated Hospital, Zhejiang University School of Medicine, Hangzhou, China.
[13]Beijing Key Lab of Mental Disorders, Beijing Anding Hospital, Capital Medical University, Beijing, China.
[14]Department of Psychiatry, University of New Mexico, Albuquerque, New Mexico, USA.
[15]Department of Psychology, Georgia State University, Atlanta, Georgia, USA.
[16]Neuroscience Institute, Georgia State University, Atlanta, Georgia, USA.
[i]ORCID ID (https://orcid.org/0000-0003-2946-1786).
*Equal contribution.

Impact Statement

This study is the first attempt that explored the temporal change on default mode network (DMN) connectivity in a relatively large cohort of patients with major depressive disorder (MDD). We also introduced a new hypothesis that explains the inconsistency in DMN functional network connectivity (FNC) comparison between MDD and healthy control based on static FNC in the previous literature. Additionally, our findings suggest that within anterior cingulate cortex connectivity and the connectivity between the precuneus and posterior cingulate cortex are the potential biomarkers for the future intervention of MDD.

Key words: default mode network; dynamic functional network connectivity; machine learning; major depressive disorder; resting-state functional magnetic resonance imaging

Introduction

Major depressive disorder (MDD) is a significant mood illness marked by emotions of sorrow, anger, loss, decreased interests, and social isolation (Fountoulakis, 2010; Otte et al., 2016). Every year, MDD affects more than 16 million people in the United States (6.7%) and 350 million adults worldwide (4.4%) (Bromet et al., 2011). Despite substantial advances in treating MDD, 20–30% of individuals remain resistant to therapy (Kraus et al., 2019). As such, we need a deeper knowledge of the underlying processes of MDD to enhance therapies. In recent decades, resting-state functional magnetic resonance imaging (rs-fMRI) studies based on functional connectivity (FC) and its network analog functional network connectivity (FNC) (Jafri et al., 2008) have been used to reveal new information about the neurophysiological substrates of MDD by identifying abnormal communication within and between functional brain regions and networks (Dichter et al., 2015; He et al., 2016, 2017; Xiao et al., 2019; Ye et al., 2015; Zeng et al., 2012; Zhu et al., 2012).

The default mode network (DMN), which consists of the anterior cingulate cortex (ACC), posterior cingulate cortex (PCC), and precuneus (PCu), has piqued researchers' attention due to its highest engagement during the task-free resting state and its possible role in revealing information about the intrinsic brain (Buckner et al., 2008). Early investigations highlighted the contribution of DMN in spontaneous and task-unrelated thought during rest in the healthy subjects (Binder et al., 1999), and a later study showed its impairment in the self-referential process in patients with MDD (Sheline et al., 2009).

Also, it has been demonstrated to play a function in the development of negative rumination and depressive symptoms in patients with MDD (Greicius et al., 2007; Hamilton et al., 2011). Hamilton and associates (2011) found an increasing level of activity in the DMN than networks activated during the task in MDD patients and its relationship with more depressive rumination and less reflective rumination. Another study predicted the suicidal behavior of depressed patients based on abnormal DMN connectivity (Zhang et al., 2016). All of these studied proved an essential role of DMN connectivity in MDD and highlighted its role in the pathology of depression.

Studies of dFNC within DMN subnodes have reported inconsistent results regarding the activity of this network in MDD. While multiple studies reported increased within DMN connectivity in MDD (Greicius et al., 2007; Hamilton et al., 2011; Li et al., 2013; Posner et al., 2016; Wang et al., 2016; Zhou et al., 2010), there have also been other studies showing less dFNC in DMN subnodes of patient with MDD (Cullen et al., 2009; Yan et al., 2019). By assuming that FNC is constant throughout time, the majority of these studies ignore the time-varying behavior of DMN FNC in MDD. Although FNC is highly dynamic even without any external inputs, DMN dFNC of MDD has not yet been comprehensively explored. dFNC has been studied in other disease groups (Allen et al., 2014; Calhoun et al., 2014; Fu et al., 2019; Vergara et al., 2018; Zhang et al., 2018).

To date, only three studies have assessed dFNC in MDD (Kaiser et al., 2016; Li et al., 2019; Wise et al., 2017; Zhi et al., 2018). Only one of those probed the alteration of DMN dFNC (between PCC and medial prefrontal cortex) by looking at the standard deviation of dFNC, although this was within a relatively small data set (Wise et al., 2017). Since it is well known that the brain is extremely active, we hypothesized that a focus on the dynamics among subnodes of the DMN would show new evidence, which cannot be observed through whole-brain FNC (Lin et al., 2017). In addition, to avoid the strong assumptions of a seed-based method to extract the network components in the brain, we used a semiblind adaptive framework called NeuroMark (Du et al., 2019).

Using replicated brain network templates extracted from two data sets with around 900 normative resting fMRI, NeuroMark provides a fully framework-based automated independent component analysis (ICA) that uses spatially controlled ICA to estimate components that are adaptable to each individual and comparable across subjects. Based on the NeuroMark template, we identified seven data-driven DMN subnodes, including ACC (two nodes), PCC (two nodes), and PCu (three nodes), and found an aberrant temporal pattern as well as a connection between this abnormal connectivity pattern and symptom intensity in patients with MDD.

To examine dFNC within the DMN in MDD, we used a sliding window method followed by *k*-means clustering to establish a collection of DMN connection states (Calhoun et al., 2014). Also, we estimated hidden Markov model (HMM) transition probabilities between dFNC states. Next, using statistical analysis on the HMM features estimated form DMN dFNC, we explored a link between abnormal DMN dFNC and symptom severity in MDD. Also, we leveraged a machine learning method to examine the DMN subnode FNC distinctions between healthy control (HC) individuals and patients with MDD in each estimated state.

Materials and Methods

The appropriate ethics committees approved this work, and informed permission was acquired from each individual before scanning, as required by each site's institutional review board.

Participant

Five hundred thirty-nine Chinese Han participants (262 patients with MDD and 277 HCs) were recruited from four Chinese hospitals: the West China Hospital of Sichuan (Site 1), the Henan Mental Hospital of Xinxiang (Site 2), the First Affiliated Hospital of Zhejiang (Site 3), and the Anding Hospital of Beijing (Site 4). The structured clinical interview for diagnostic (SCID-P) and statistical manual of mental disorders confirmed depression in individuals with MDD, and SCID/NP confirmed the absence of a psychiatric diagnosis for HCs. In addition, HCs with any psychiatric disorder history in their first-degree relatives were excluded. The 17-item Hamilton Depressive Rating Scale (HDRS) assessed the current symptom severity of MDD subjects (Hamilton, 1960).

Data acquisition

In Site 1, a 3T Philips scanner (Achieva, Netherlands) with an 8-channel phased-array head coil was used for collecting the functional images. Repetition time (TR)/echo time (TE) = 2000/30 msec, field of view (FOV) = 240 × 240 mm (64 × 64 matrix), flip angle (FA) = 90°; 38 sequential ascending axial slices of 4 mm thickness and 0 mm gap were the parameters used in this process. For Site 2, a total of 240 volumes of echo-planar images were collected using a 3T Siemens scanner (Verio, Germany) with a 12-channel phased-array head coil and TR/TE = 2000/30 msec, FOV = 220 × 220 mm (64 × 64 matrix), FA = 90; 33 sequential ascending axial slices of 4 mm thickness and 0.6 mm slice gap. Site 3 used a 3T Siemens scanner (Prisma, Germany) with a 12-channel phased-array head coil for acquiring the fMRI data. The scanning parameters were TR/TE = 2000/30 msec, FOV = 220 × 220 mm (64 × 64 matrix), FA = 90°, 38 sequential ascending axial slices of 4 mm thickness and 0 mm slice gap. For Site 4, a 3T Siemens scanner (Prisma) with a 32-channel phased-array head coil was used. In this site, the scanning parameters were TR/TE = 2000/30 msec, FOV = 220 × 220 mm (64 × 64 matrix), FA = 90°, 38 sequential ascending axial slices of 4 mm thickness and 0.7 mm gap. Foam pads and earplugs were utilized to reduce head movement and scanner noise during scanning, and individuals were told to close their eyes and stay awake throughout the resting-state scan.

Data processing

In the MATLAB2019 environment, the fMRI data were preprocessed using statistical parametric mapping (SPM12). Before preprocessing, the first five mock scans were deleted. On the fMRI data, we performed slice-timing correction before using rigid body motion correction to adjust subject head motion. After that, we resampled to $3 \times 3 \times 3\ mm^3$ using an echo-planar imaging template in the standard Montreal Neurological Institute (MNI) space. Finally, we smoothed the fMRI images using a Gaussian kernel having a full-width at half-maximum (FWHM) of 6 mm.

We employed the NeuroMark fully automated ICA process, which leverages previously obtained component maps as priors for spatially restricted ICA, to extract trustworthy independent components or independent components (ICs) (Du et al., 2019). Replicable components were identified in NeuroMark by comparing group-level spatial maps obtained from two large HC data sets. If they show peak activations in the gray matter,

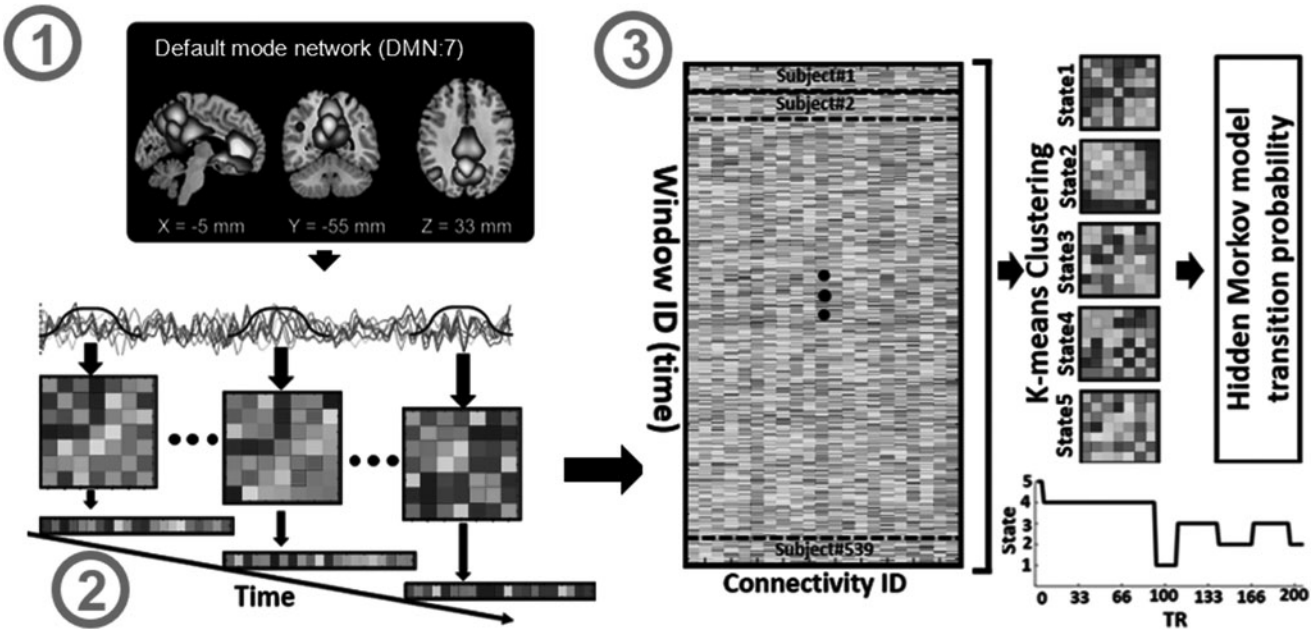

FIG. 1. Analytic pipeline. Step 1: The time-course signal of seven subnodes in the DMN has been identified using group-ICA. Step 2: After identifying seven subnodes in DMN, a taper sliding window was used to segment the time-course signals and then calculated the dynamic functional network connectivity (dFNC). Each subject has 205 FNCs with a size of 7 × 7. Step 3: After vectorizing the FNC matrices, we have concatenated them, and then a *k*-means clustering with correlation as distance metrics was used to group FNCs to five distinct clusters. Then, based on the state vector, we calculated between-state transition probability or HMM features for each subject. In total, 25 features were estimated from the state vector of each subject. DMN, default mode network; FNC, functional network connectivity; HMM, hidden Markov model; ICA, independent component analysis.

Table 1. Component Labels Extracted Using NeuroMark

Component name	*Peak coordinate (mm)*		
(IC 32), Precuneus [PCu1]	−8.5	−66.5	35.5
(IC,40), Precuneus [PCu2]	−12.5	−54.5	14.5
(IC 23), Anterior cingulate cortex [ACC1: pACC]	−2.5	35.5	2.5
(IC 71), Posterior cingulate cortex [PCC1]	−5.5	−28.5	26.5
(IC 17), Anterior cingulate cortex [ACC2: sgACC]	−9.5	46.5	−10.5
(IC 51), Precuneus [PCu3]	−0.5	−48.5	49.5
(IC 94), Posterior cingulate cortex [PCC2]	−2.5	54.5	31.5

ACC, anterior cingulate cortex; pACC, posterior ACC; sgACC, subgenual ACC.

have limited spatial overlap with known vascular, ventricular, motion, and susceptibility artifacts, and have prominent low-frequency fluctuations on their time-courses, a selection of matching components was selected as significant. Seven ICs including three components of the PCu, two components of the ACC, and two components of the PCC identified within the DMN (Fig. 1; Step 1). In addition, Table 1 shows all the seven components (regions) and their peak coordinates used in this study.

Dynamic functional connectivity

The dFNC of the seven subnodes of DMN was calculated using a sliding window method for each participant $i = 1 \ldots N$, as illustrated in Figure 1. To localize the data set at each time point, a tapered window was created by convolving a rectangle (window size = 20 TRs = 40 sec) with a Gaussian (= 3 sec). To quantify the dFNC between seven subnodes in the DMN, the correlation matrix was calculated using windowed data. Twenty-one connectivity features were estimated out of seven subnodes in DMN. The changes in brain connectivity between DMN subnodes as a function of time were formed by concatenating dFNC estimates of each window for each subject to produce an $(C \times C \times T)$ array (where $C = 7$ represents the number of DMN subnodes, and $T = 205$ indicates the number of windows), as shown in Step 2 of Figure 1 (Allen et al., 2014; Calhoun et al., 2014; Fu et al., 2019).

Clustering and latent transition probability feature estimation

In the next step, we concatenated the dFNC of all participants as shown in Step 3 of Figure 1 and applied a *k*-means clustering method to these dFNC windows to put them into a set of separated (Sendi et al., 2021). The elbow criterion, which is based on the ratio of inside to between cluster distance, was used to determine the optimal number of centroid states (Li and Zoltàn, 2017). The best number of clusters was calculated to be five in a search window of *k* from three to eight. In addition, the correlation distance metric, due to its sensitivity to connectivity patterns regardless of magnitude, was used in the *k*-means clustering method with 1000 repetitions (Damaraju et al., 2014). *k*-means clustering produces five unique states for each group, as well as a state vector for each participant. A state vector depicts how the network evolves over time between any two states. Next, we computed the transition probability from one state to another based on each subject's state vector and utilized this as a latent of dFNC. In this model, the probability of transitioning from state *j* at time *t* to state *i* at time step *t + 1* is denoted by a_{ij} (Step 3 in Fig. 1).

$$a_{ij} = p(s(t+1) = i | s(t) = j). \quad (1)$$

N states resulted in N^2 between-state transition probabilities or HMM features. Therefore, with 5 states, 25 features were estimated using the HMM for each subject.

Quantifying group difference using the feature selection method

A logistic regression (LR) was utilized to classify the two groups based on their connectivity characteristics, which are 21 features (i.e., C_1, C_2, …, C_{21}) in total, as shown in Figure 2, to quantify the DMN FNC difference between MDD and HC in each state. It is worth mentioning that with seven subnodes in DMN, we calculated 21 connectivity features, each of which indicates the degree of connection between any two DMN subnodes. In contrast to statistical learning, which examines each feature individually and ignores the interplay of input features, the machine learning-based feature selection technique would provide a generalized model of the difference between HC and MDD characteristics (Bzdok et al., 2018). We used leave-one-site nested cross-validation (CV), in which all participants from one site were used for testing and the other three sites were used for training (Wainer and Cawley, 2018). We used this approach for training and testing to evaluate the effect scanning site, and with four sites, we did this process four times. In any outer fold of the CV, the data were split into training and test sets. In an inner fold, the training data were separated into another training and validation data. The optimal parameters were estimated by training multiple models with inner-loop training data and then validating them with the validation data set. The hyperparameters of each model are set in this procedure to reduce the generalization performance's inner-fold CV error.

We then utilized elastic net regularization (ENR) as a feature learning approach to select a subset of features that are most important to the classification of MDD versus HC. We chose to use ENR rather than least absolute shrinkage and selection operator or LASSO with *L1*-penalization since ENR used both *L1*-and *L2*-penalization in Equations (2) and (3) (Tibshirani, 2011; Zou and Hastie, 2005), while LASSO depends only on L1. Elastic net is a regularization and feature selection technique that estimates the model parameters of the LR and selects the most important features by minimizing a cost function. This method would drive the model parameters (i.e., feature coefficients) toward zero while λ increases. This would result in a model parameter trajectory as a function of and a regularization path for the model. The feature associated with the slowest declining coefficients was considered the most significant. The cost function used in ENR is shown in the equations below:

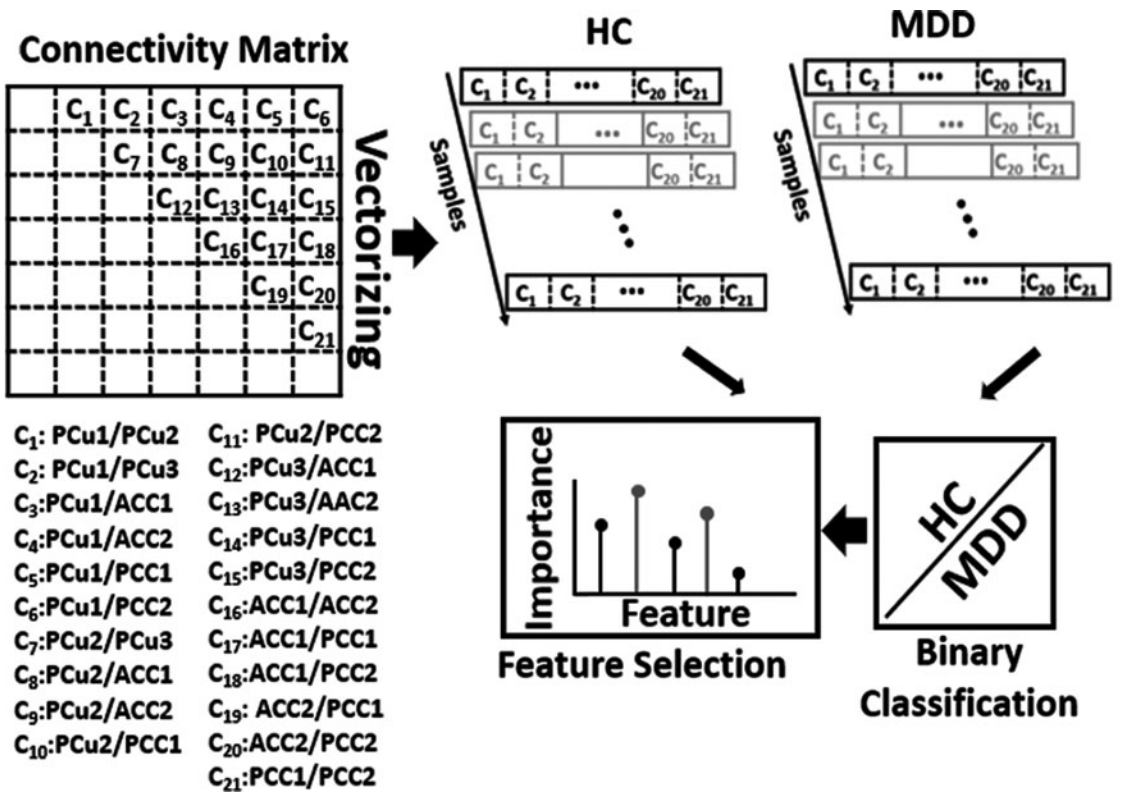

FIG. 2. Classification between MDD and HC and feature selection based on 21 features in each state. The 21 connectivity features that estimated from 7 subnodes in the DMN were used as input to fit an LR as a classifier to discriminate MDD from HC in each state. Feature selection used the model generated by LR to find a subset of features that significantly contributed to discriminating between two classes. The relative retained proportion of the features was compared using a one-way ANOVA, which found that they were a statistically significant predictor of feature contribution in the model. To account for the site's variation, we trained an LR model from the subjects of three sites and tested that model on the remaining site. We repeated this process four times to cover all four sites. ANOVA, analysis of variance; HC, healthy control; LR, logistic regression; MDD, major depressive disorder.

$$\min_{\beta_0,\beta}\left(\frac{1}{2N}\sum_{i=1}^{N}\left(y_i-\beta_0-x_i^T\beta\right)^2+\lambda P_a(\beta)\right). \quad (2)$$

$$P_a(\beta)=\frac{(1-\alpha)}{2}\beta_2^2+\alpha|\beta|_1, \quad (3)$$

where N is the number of samples, y_i is the label of sample i, x_i is the feature vector of sample i, β and β_0 are model parameters, λ is the regularization parameters, and $P_a(\beta)$ is the penalty term in which α, is a scaler value, determines the contribution of *L1* or *L2* norms, in which $\alpha=1$ keeps only the *L1* and $\alpha=0$ keep only the *L2* norm (Zou and Hastie, 2005). In this study, the α was 0.95.

We evaluated the proportion of models for which a particular parameter was kept during the sweep of the model parameters in the inner fold to find the most relevant feature in the classification between MDD and HC. The contribution of each feature in the categorization of two groups was shown by this assessment. A one-way analysis of variance (ANOVA) was used to examine the relative retained proportion of the features, which revealed that they were a statistically significant predictor of feature contribution in the model. We selected those features that have the highest equal involvement in the feature learning process based on multiple comparison tests on the one-way ANOVA (Hochberg, 1987).

Statistical analyses

We utilized a partial correlation with the Pearson technique and accounting for age, gender, and scanning locations to discover a relationship between HMM characteristics and HDRS in the MDD group. On all 25 HMM features, we ran all statistical analyses. The Benjamini–Hochberg correction technique was used to modify all p-values for the false discovery rate (FDR) correction. We also performed repeated comparisons using a one-way ANOVA test to determine the most important feature in ENR (Hochberg, 1987).

Results

Demographic and clinical characteristics

Table 2 shows the demographic and clinical features of the participants based on their site. We did not detect a significant age or gender difference between HC and MDD using a Kolmogorov–Smirnov two-sample test on all individuals combining all sites. However, the age difference between MDD and HC subjects was significant within Site 4 only. Across all MDD patients, the mean and the standard deviation of the HDRS were 19.32 and 7.35, respectively.

The dynamic connectivity states

Five different DMN dFNC states identified by the k-means clustering algorithm are shown in Figure 3a. We observed

Table 2. Demographic and Clinical Details of the Subjects for Each Site

		MDD	*HC*	*p*
Site 1	Number	70	70	NA
	Age (year) (mean ± SD)	33.29 ± 10.63	33.24 ± 10.48	0.95
	Gender (M/F)	24/46	25/45	0.99
	HDRS (mean ± SD)	23.35 ± 7.17	NA	NA
	Duration of illness (month) (mean ± SD)	38.13 ± 50.63	NA	NA
Site 2	Number	78	110	NA
	Age (year) (mean ± SD)	29.03 ± 9.95	26.95 ± 10.08	0.41
	Gender (M/F)	27/51	34/76	0.99
	HDRS (mean ± SD)	21.47 ± 6.75	NA	NA
	Duration of illness (month) (mean ± SD)	28.35 ± 45.84	NA	NA
Site 3	Number	85	68	NA
	Age (year) (mean ± SD)	35.43 ± 12.87	35.92 ± 12.73	0.73
	Gender (M/F)	38/47	30/38	0.99
	HDRS (mean ± SD)	14.64 ± 8.54	NA	NA
	Duration of illness (month) (mean ± SD)	84.63 ± 95.19	NA	NA
Site 4	Number	29	29	NA
	Age (year) (mean ± SD)	35.13 ± 9.02	29.89 ± 7.34	0.04
	Gender (M/F)	11/18	12/17	0.99
	HDRS (mean ± SD)	17.57 ± 5.9	NA	NA
	Duration of illness (month) (mean ± SD)	NA	NA	NA
Total	Number	262	277	
	Age (year) (mean ± SD)	32.91 ± 11.07	31.05 ± 10.66	0.061
	Gender (M/F)	100/162	101/176	0.68
	HDRS (mean ± SD)	19.32 ± 7.35	NA	NA
	Duration of illness (month) (mean ± SD)	51.81 ± 69.15	NA	NA

All *p*-values have been calculated using the two-sample Kolmogorov–Smirnov test.
HC, healthy control; HDRS, Hamilton Depression Rating Scale; MDD, major depressive disorder; NA, not applicable; SD, standard deviation.

various connectivity patterns in these five estimated states. States 2, 4, and 5 showed more positive connectivity in PCu regions. However, we observed less connectivity in three PCu regions in States 1 and 3. State 4 was the only one that showed negative connectivity in ACCs. Also, States 2, 3, and 4 showed positive connectivity at PCCs, and other states showed negative connectivity in these subnodes of DMN. State 2 was the only one that showed less connectivity between ACC and other regions in DMN. In addition, States 2 and 4 showed more positive connectivity between PCu and

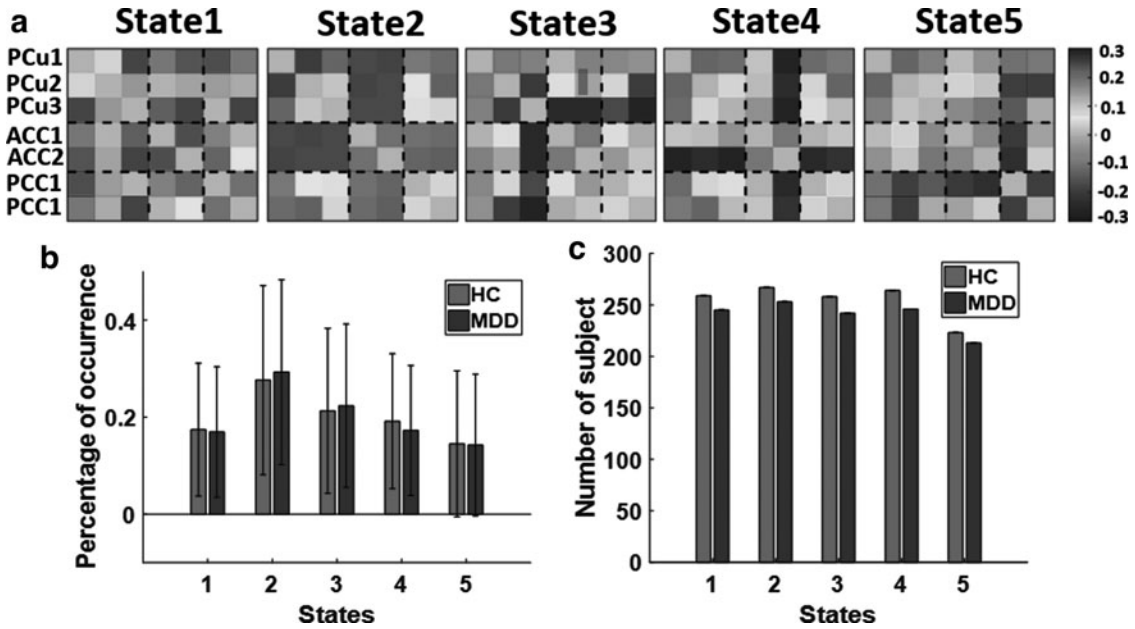

FIG. 3. Dynamic connectivity state results. **(a)** The five identified dFNC states using the *k*-means clustering method. **(b)** The group difference between HC (red) and MDD (blue) in the percentage of occurrence in each state. No significant difference was observed between the two groups. **(c)** The number of HC and MDD subjects in each state. dFNC, dynamic functional connectivity.

PCC. However, other states showed both positive and negative connectivity between PCu and PCC. We computed the percentage of occurrence of each dFNC across all subjects. The results are shown in Figure 3b for MDD and HC subjects. To compare the percentage of occurrence of HC and MDD groups, we used a two-way ANOVA test, and we did not see any substantial difference between patients with MDD and HCs. Besides, Figure 3c shows the number of MDD and HC participants of each state. It is worth noting that not all participants have dFNC windows assigned to each of the five states in Figure 3a.

Difference between HC and MDD connectivity feature of each state

We used the connectivity features, in total, 21 features obtained from seven subnodes of DMN, to compare HC and MDD in each state. Each feature demonstrated the degree of connection between any two DMN subnodes. We used a fourfold (leave-one-site-out) CV LR classifier with the ENR feature selection algorithm and modeled the distinction between HC and MDD groups in each state. Figure 4a shows the feature contribution in the classification between HC and MDD (with a mean area under the curve or AUC of 0.57) in State 1. The normalized occurrences of connectivity feature in this classification are shown in this figure. Purple indicates features preserved by the ENR that were substantially more common than the average inclusion rate. As this figure shows, C_{11}, C_{15}, C_{16}, and C_{18} were equally the most important features in the classification between HC and MDD in this state. In addition, Figure 4a (right panel) shows the group distinctions between patients with MDD and HC participants in the strength of those connectivity features selected by ENR. When comparing MDD patients with HCs, the red lines show increased connection and the blue lines represent decreased connectivity. In addition, the wider line means larger group differences. As this figure shows, HCs had stronger connectivity between PCu (including PCu2 and PCu3) and PCC. Also, the connectivity between ACC1 and ACC2 was less in HCs than that in MDD subjects in this state. In addition, the connectivity between ACC and PCC was higher in HCs than that in MDDs. Based on the feature selection results, we did not observe any major discrepancies between MDD and HC in the connectivity within PCus and within PCCs.

The normalized occurrences of connectivity features in the classification between HC and MDD of State 2 are shown in Figure 4b. In this classification, using a fourfold CV, the mean value of the classification AUC was 0.64. As this figure shows, the contribution of C_{10}, C_{11}, and C_{14} was significantly and equally higher than other features. Also, we found that the connectivity between PCu2 and PCC2, and the connectivity between PCu3 and PCC1 were higher in HC subjects. While the connectivity between PCC1 and PCu2 was lower in HC subjects. Therefore, overall, we observed more connectivity between the PCu and PCC in HC than MDD subjects in this state. No significant difference between MDD and HC was observed in within-region connectivity in this state. Interestingly, compared with other states, no significant difference between ACC nodes was observed in this state.

The feature selection result in the classification between HC and MDD of State 3 is shown in Figure 4c, where the AUC of classification was 0.58 in a fourfold CV. In this classification, the C_1, C_2, C_{14}, C_{16}, and C_{18} were equally the most important features, differentiated between HC and MDD. In this state, we observed weaker connectivity within PCu (i.e., PCu1, PCu2, and PCu3) regions and within ACC (i.e., ACC1 and ACC2) regions in HC subjects. Also, we found a stronger connectivity between the connectivities between PCu3 and PCC1 and between ACC1 and PCC2 of HC subjects in this state. This was the only state that showed a difference between MDD and HC subjects in the connectivity among PCu nodes.

Figure 4d shows those features that were retained by the ENR equally and significantly more frequently than other features in the classification between HC and MDD in State 4. In this classification, the mean AUC of fourfold CV was 0.57, and C_{11}, C_{16}, and C_{17} had the strongest contribution compared with other features. In this state, the connectivity within ACC regions and between PCu2 and PCC2 was higher in HC subjects. Also, the connectivity between ACC1 and PCC1 was less in this group. This state is the only state that showed a higher connectivity within ACC nodes in HC subjects.

Finally, the result of feature learning in the classification between HC and MDD of State 5, in which the mean value of fourfold CVAUC was 0.59, is shown in Figure 4e. Among all connectivity features, only C_5, C_{11}, and C_{16} showed significant and equal contributions in this classification. In State 5, the PCu and PCC connectivity was stronger in HCs, and the connectivity of ACC was weaker in these subjects.

Behavioral correlation with HMM features

The next important question was how DMN between-state transition features (or HMM) are correlated with symptom severity. To answer this question, we estimated the Pearson's linear correlation and HDRS between-state transition probability, that is, a_{ij}, while adjusting for age, gender, and scanning site. The correlation between HDRS and state transition probability and their associated FDR-corrected p-values are shown in Figure 5a. With 25 HMM features, we had 25 correlations and their associated p-values, as shown in this figure. Based on this analysis, only one correlation between HDRS and the state transition feature was significant after correcting for multiple comparisons (FDR-corrected $p < 0.05$). We found that symptom intensity had a positive link with state transition from State 4 to State 3 ($r = 0.19$, FDR-corrected $p = 0.04$, $n = 234$), as shown in Figure 5b. In other words, the transition from State 4, which showed higher connectivity between PCu and PCC and lower ACC connectivity, to State 3 with lower connectivity between PCu and PCC and higher ACC connectivity, increased by symptom severity.

It is worth noting that certain patients, as illustrated in Figure 5b, do not have a transition from State 4 to State 3. To explore whether these subjects would drive the result or not, we removed these subjects and repeated the correlation analysis. As expected from the graph, after removing those subjects, the correlation values increased and became more significant. The corrected p-value changed from ($r = 0.19$) 0.04 to ($r = 0.33$) 0.02. Overall, removing those subjects with zero transition probability increases the correlation between the transitions from State 4 to State 3 with symptom severity.

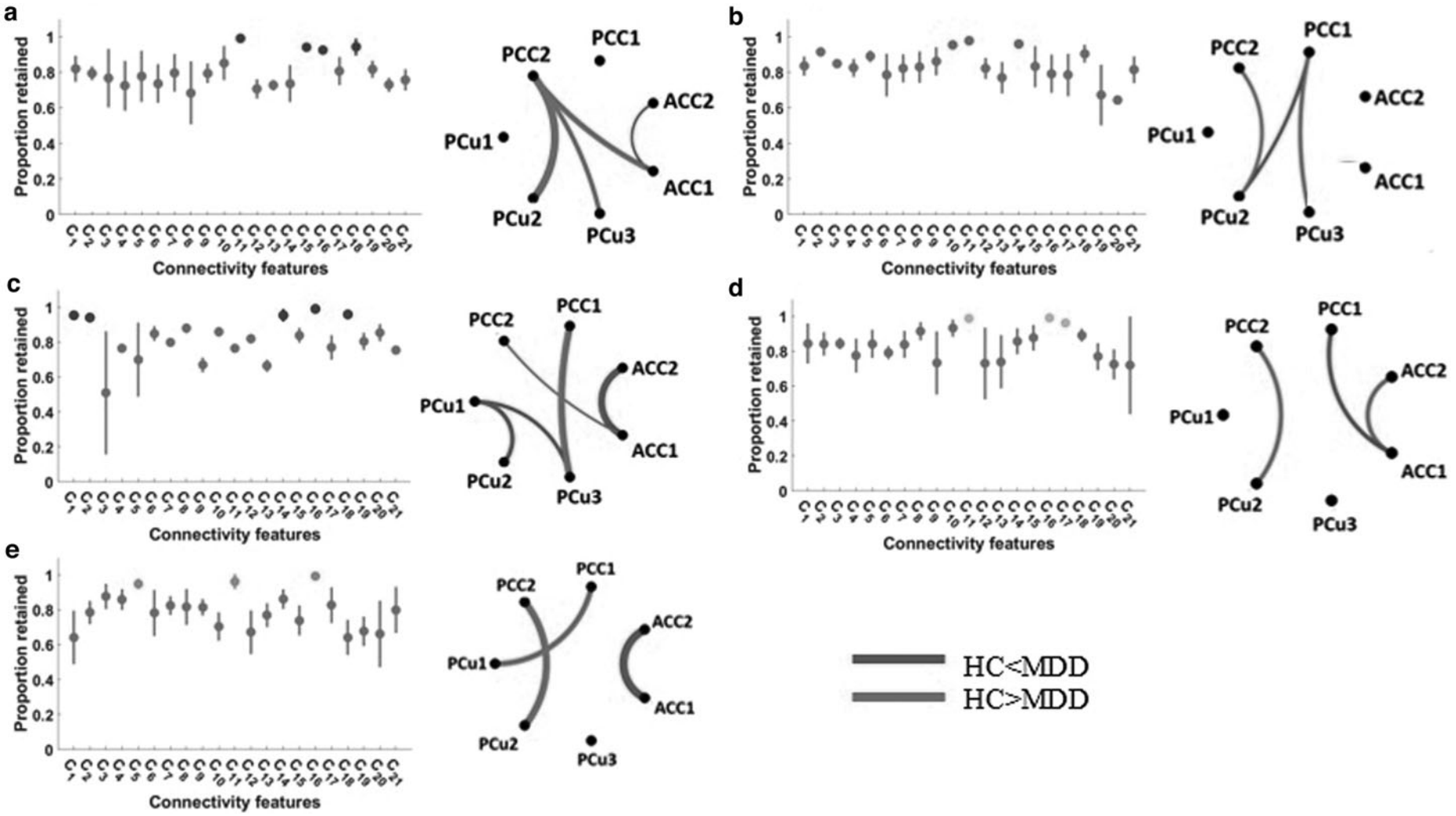

FIG. 4. Difference between MDD and HC connectivity in each state. The distribution of biomarkers identified by ENR. Features that were retained significantly more than the overall mean are shown in color (left panels). The group difference visualization of dFNC in each state is shown in the right panel. In this graph, a wider line means a larger group difference. Red lines represent increased connectivity, while blue lines represent decreased connectivity in HC patients compared with MDD patients (right panels). **(a)** Feature selection and group difference results in State 1, **(b)** feature selection and group difference results in State 2, **(c)** feature selection and group difference results in State 3, **(d)** feature selection and group difference results in State 4, **(e)** feature selection and group difference results in State 5. ENR, elastic net regularization.

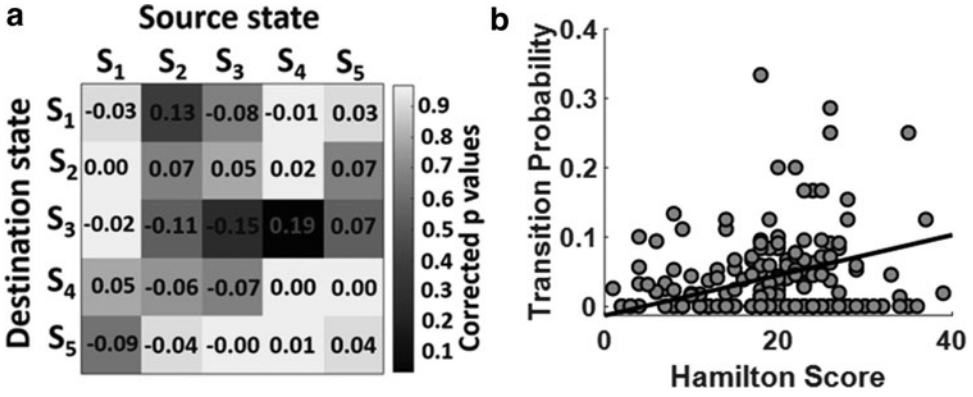

FIG. 5. Behavioral correlation with HMM features. **(a)** The partial correlation between HDRS and twenty five between-state transition probabilities or HMM features while controlling for age, gender, and scanning site (FDR-corrected $p < 0.05$). Color bar represents the corrected p-value (FDR corrected $p < 0.05$). Only the transition from State 4 to State 3, that is, a_{34}, showed a significant correlation with symptom severity after FDR correction. **(b)** The correlation between HDRS and a_{34} ($r = 0.19$, FDR-corrected $p = 0.04$, $n = 234$). The transition from State 4 to State 3 increases by the severity of symptoms. FDR, false discovery rate; HDRS, Hamilton Depressive Rating Scale.

Discussion

In this study, using a very large sample size, we examined the changes in FNC dynamics during rs-fMRI between healthy people and people with MDD. To this end, we framed our approach around three main questions: (1) what are the dFNC reoccurring patterns across time and across subjects? (2) What is the difference between dFNC of MDD and HC subjects in each of these patterns? (3) How do the temporal properties of these patterns correlate with symptoms severity?

For the first question, we found a disrupted pattern within and between the connectivities of PCu, ACC, and PCC subnodes. We noticed both negative and positive connectivities in PCC and ACC. Also, within PCu connectivity was stronger in States 2, 4, and 5 than that in States 1 and 3. Our work goes beyond previous research by incorporating the dynamics of DMN FNC using data-driven subnodes and shows that FNC within DMN subnodes is indeed highly dynamic, representing a higher activity and flexibility in functional coordination in this mode. While at least one prior research used predefined regions of focus to assess DMN dynamics (Wise et al., 2017), there has not been a method that compares the state connectivity difference between patients and controls and links the between-state transition probability with symptom severity using data-driven DMN subnodes. As recent research has shown, it is critical to verify that the data within the node are consistent; otherwise, the findings may be skewed or deceptive (Yu et al., 2017) or inconsistent (Yan et al., 2019). This is particularly true when looking at dynamics (Iraji et al., 2020).

Using DMN static FNC data, previous literature has reported inconsistent results in within DMN subnode connectivity by showing both increases (Greicius et al., 2007; Hamilton et al., 2011; Li et al., 2013; Posner et al., 2016; Wang et al., 2016; Zhou et al., 2010) and decreases (Cullen et al., 2009; Yan et al., 2019), and even no significant difference between MDDs and HCs (Pannekoek et al., 2014) in the connectivity of this network. Although this inconsistency could be due, in part, to disparities in disorder subpopulations or symptoms and even small sample size as Yan and associates (2019) claimed, we assume that the heterogeneousness is partially constrained by the focus on static FNC, achieved from the correlation within the whole time series. The current study, which showed a disrupted (i.e., both increase and decrease) pattern within connectivity of DMN, provides a more natural analytic approach, enabling us to focus on the dynamics of the network over a shorter time span. In addition, as Yan and associates (2019) claimed, another reason for having inconsistent results in comparing the DMN connectivity between MDD and HC in the previous literature is using different preprocessing parameters. Our usage of NeuroMark, a replicable platform for extracting the subnodes within DMN, was developed to address this issue (Du et al., 2019).

We cast the second question into a classification problem to differentiate between HC and MDD subjects in each state. We trained an LR with ENR as an embedded feature learning to find the essential connectivity features in grouping HC and MDD subjects. Using the feature learning method, we found that the connectivity between PCu and PCC is one of the most important features that can differentiate between HC and MDD in all states. Also, we found that the connectivity between PCC and PCu is relatively lower in MDD patients than that in HC subjects.

Previous studies showed more activation in PCu, and PCC plays a vital role in self-reflective thinking, the main feature of depression (Cavanna and Trimble, 2006). In another study, the activity in PCu and PCC was decreased by disrupting normal neural circuitry in the medial parietal region using transcranial magnetic stimulation, which caused a decrease in self-references (Lou et al., 2004). In addition, more activation in PCu/PCC has been reported during the evaluation of self-referential pleasantness (Perrone-Bertolotti et al., 2016). In addition, a prior study found reduced functional connection between PCC and PCu in the first episode of treatment-naive individuals (Zhu et al., 2012). By analyzing the dFNC of DMN, the current study offers new evidence on the PCu and PCC connectivity in patients with MDD and further supports the PCC and PCu connectivity role in the pathogenesis of MDD.

Also, results showed that within-ACC connectivity (i.e., the connectivity between ACC1 and ACC2) contributes in MDD and HC classification for all states except State 2. Using the anatomical model (Tzourio-Mazoyer et al., 2002), we found that ACC1 is posterior ACC or pACC, and ACC 2 is subgenual ACC or sgACC (Table 1). The ACC region is involved in integrating neuronal circuitry for the management of uncomfortable emotions (Etkin et al., 2012; Stevens et al., 2011). Several years of studies proved a substantial role of ACC subregion, particularly sgACC, in the pathology of MDD. For many years, sgACC has been the main deep brain stimulation (DBS) target for producing prolonged remission from depression (Mayberg et al., 2005).

A previous study found ACC hyperactivity during sorrow in healthy subjects (George et al., 1995). Also Greicius and associates (2007) reported a higher sgACC connectivity in patients with MDD compared with HC individuals. Recently, a study reported a positive link between the sgACC and dorsal ACC connectivity and the persistence of sadness and inflexibility of daily emotions in both HCs and patients with MDD (Schwartz et al., 2019). However, the same study also showed a reduced connectivity in ACC for MDD versus HC. In addition, Cullen and colleagues (2009) showed a decrease in sgACC connectivity in MDD patients. This discrepancy may be attributable to an emphasis on static functional connection while neglecting the extremely dynamic nature of these subnodes. In our current study, in three states out of five, we observed increased FNC within ACC (i.e., between sgACC and pACC) in MDD subjects. In addition, we found that within ACC connectivity is more in HC subjects in State 4, and this connectivity does not show a considerable distinction between MDD and HC in State 2. An aberrant spatiotemporal pattern in the connectivity between two ACC subregions potentially stressed out the importance of studying dFNC, and evaluating the connectivity is a shorter timescale. This abnormal pattern possibly can explain why previous studies based on static FNC reported inconsistent (both increase and decrease) results within ACC connectivity in MDD versus HC.

Also, we noticed a disordered spatiotemporal pattern in the connectivity between ACC1 (or pACC) and PCC by showing a lower MDD FNC for State 1 and State 3 and a higher MDD connectivity in State 4. In addition, no major difference between patients with MDD and HC is observed in State 2 and State 5. This disrupted pattern of pACC and PCC connectivity in the gap between MDD and HC potentially marks the importance of analyzing FNC in a shorter period and suggests further prospective investigation in the connectivity between ACC and PCC in MDD.

For the last question, first, we estimated the HMM transition probability and model the temporal alterations of dFNC. We found a significant positive link between the transition from a state with high PCu/PCC (the connectivity between PCu and PCC) and low ACC connectivity to a state with lower PCu/PCC connectivity and higher ACC and symptom severity. These results provide more evidence about the role of connectivity between PCu and PCC and the connectivity in ACC as a biomarker of MDD, and this role is higher in severe MDD. Recent studies on Alzheimer's disease found a relationship between the number of switches among states and symptom severity (Fiorenzato et al., 2019). Here we used between-state transition probability from the HMM, which mathematically is different from the study as mentioned above, and for the first time found a correlation between MDD symptom severity and HMM features. In the current study, we introduced HMM features as a potential biomarker that possibly can elucidate some underlying mechanism in patient symptom variation and its association with the temporal pattern of DMN connectivity. Besides, quantification of the link between symptom severity and HMM features (and in the general dynamic pattern) in MDD patients potentially leads to an optimized treatment and also prognostic of MDD, which needs future investigation.

The DMN has been a main target for DBS and noninvasive neuromodulation such as repetitive transcranial magnetic stimulation (rTMS) for many years. Recently, a study proved that rTMS reduces the FNC within DMN (Liston et al., 2014). Instead, the state-dependent stimulation showed more efficiency than the blind stimulation in which we do not account for the state of the brain at the stimulation onset (Schiena et al., 2020; Silvanto and Pascual-Leone, 2008; Widge et al., 2018). However, it remains unclear which biological properties should be used as the most appropriate control signal and what is the target brain state for stimulation (Bergmann, 2018). In our study, we introduce ACC connectivity and the connectivity between PCu and PCC as a potential marker to control and optimize the stimulation parameters. Our results suggest a potential value of applying the stimulation during the state with higher ACC connectivity and lower PCu/PCC connectivity and changing that state to a state with lower ACC and higher PCu/PCC connectivity. Also, the between-state transition probability is another marker that can be used as a control signal in the closed-loop stimulation. In a closed-loop therapy, we should reduce the shift likelihood from a state with lower ACC and higher PCu/PCC connectivity to another one with higher ACC and lower PCu/PCC connectivity. There are of course many technical limitations for implementing a real-time system that can calculate and find brain FNC states and administering TMS while we collect fMRI data (Monti et al., 2017). However, the results imply a possible value of moving in this direction.

Limitations

Although rge HDRS is widely used in scaling the symptom severity of depression, this score is very reliant on the skill of the interviewer (Sharp, 2015). Since the data in this study are coming from four different sites with different raters, this might add a variation and error for HDRS values across sites. In addition, this score is heavily focused on somatic symptoms, and previous studies questioned its reproducibility across studies (Bagby et al., 2004). The size of the window is an implicit assumption about the dynamic behavior in that a smaller window catches more fast fluctuations, while a larger window smoothes out the oscillations more. More study can be done in the future to analyze the whole spectrum of dynamics. Furthermore, prospective research in various feature selection techniques is required to confirm the repeatability of feature learning findings (Chun et al., 2020).

Conclusion

Prior studies on static FNC have demonstrated that the DMN plays an essential role in MDD. We expand this body of knowledge into the dynamic world in the study presented here, looking at how time-varying features of DMN

connectivity relate to MDD and symptom severity. We found that in shorter timescale estimates, patients with MDD exhibit lower connectivity between PCu and PCC and have long been associated with reflective thinking. Similarly, consistent with earlier static FNC studies identifying a relationship between ACC connectivity and persistent sadness, in our time-resolved connectivity estimates, MDD patients exhibited elevated ACC connectivity. Furthermore, patients with more severe symptoms are more likely to switch from a state of greater PCu/PCC (connection between PCu and PCC) connectivity and lower ACC connectivity to a state of lower PCu/PCC connectivity and higher ACC connectivity. Ours is the first research of DMN dFNC in a large MDD sample that shows evidence of abnormal time-varying activity in the DMN and a relationship between this abnormal activity and the severity of symptoms in this disorder group.

Author Disclosure Statement

No competing financial interests exist.

Funding Information

This work was supported by the National Institute of Health under R01EB006841, R01EB020407, R01MH121246, R01MH117107, R01MH118695, and U01MH111826.

References

Allen EA, Damaraju E, Plis SM, et al. 2014. Tracking whole-brain connectivity dynamics in the resting state. Cereb Cortex 24:663–676.

Bagby RM, Ryder AG, Schuller DR, et al. 2004. The Hamilton Depression Rating Scale: has the gold standard become a lead weight? Am J Psychiatry 161:2163–2177.

Bergmann TO. 2018. Brain state-dependent brain stimulation. Front Psychol 9:1–4.

Binder JR, Frost JA, Hammeke TA, et al. 1999. Conceptual processing during the conscious resting state: a functional MRI study. J Cogn Neurosci 11:80–93.

Bromet E, Andrade LH, Hwang I, et al. 2011. Cross-national epidemiology of DSM-IV major depressive episode: EBSCOhost. BMC Med 9:90.

Buckner RL, Andrews-Hanna JR, Schacter DL. 2008. The brain's default network: anatomy, function, and relevance to disease. Ann N Y Acad Sci 1124:1–38.

Bzdok D, Altman N, Krzywinski M. 2018. Points of Significance: statistics versus machine learning. Nat Methods 15:233–234.

Calhoun VD, Miller R, Pearlson G, et al. 2014. The Chronnectome: time-varying connectivity networks as the next frontier in fMRI Data Discovery. Neuron 84:262–274.

Cavanna AE, Trimble MR. 2006. The precuneus: a review of its functional anatomy and behavioural correlates. Brain 129: 564–583.

Chun JY, Sendi MSE, Sui J, et al. 2020. Visualizing functional network connectivity difference between healthy control and major depressive disorder using an Explainable Machine learning Method. In: 42nd Annual International Conference of the IEEE Engineering in Medicine and Biology Society (EMBC), Montreal, QC, Canada: IEEE; 1424–1427. https://ieeexplore.ieee.org/document/9175685

Cullen KR, Gee DG, Klimes-Dougan B, et al. 2009. A preliminary study of functional connectivity in comorbid adolescent depression. Neurosci Lett 460:227–231.

Damaraju E, Allen EA, Belger A, et al. 2014. Dynamic functional connectivity analysis reveals transient states of dysconnectivity in schizophrenia. Neuroimage 5:298–308.

Dichter GS, Gibbs D, Smoski MJ. 2015. A systematic review of relations between resting-state functional-MRI and treatment response in major depressive disorder. J Affect Disord 172:8–17.

Du Y, Fu Z, Sui J, et al. 2020. NeuroMark: An automated and adaptive ICA based pipeline to identify reproducible fMRI markers of brain disorders. NeuroImage: Clinical 28: 102375. www.sciencedirect.com/science/article/pii/S2213158220302126

Etkin A, Egner T, Kalisch K. 2012. Emotional processing in anterior cingulate and medial prefrontal cortex. Trends Cogn Sci 15:85–93.

Fiorenzato E, Strafella AP, Kim J, et al. 2019. Dynamic functional connectivity changes associated with dementia in Parkinson's disease. Brain 142:2860–2872.

Fountoulakis KN. 2010. The emerging modern face of mood disorders: a didactic editorial with a detailed presentation of data and definitions. Ann Gen Psychiatry 9:1–22.

Fu Z, Tu Y, Di X, et al. 2019. Transient increased thalamic-sensory connectivity and decreased whole-brain dynamism in autism. Neuroimage 190:191–204.

George MS, Ketter TA, Parekh PI, et al. 1995. Brain activity during transient sadness and happiness in healthy women. Am J Psychiatry 152:341–351.

Greicius MD, Flores BH, Menon V, et al. 2007. Resting-state functional connectivity in major depression: abnormally increased contributions from subgenual cingulate cortex and thalamus. Biol Psychiatry 62:429–437.

Hamilton JP, Furman DJ, Chang C, et al. 2011. Default-mode and task-positive network activity in major depressive disorder: implications for adaptive and maladaptive rumination. Biol Psychiatry 70:327–333.

Hamilton M. 1960. A rating scale for depression. J Neurol Neurosurg Psychiatry 56–63.

He H, Sui J, Du Y, et al. 2017. Co-altered functional networks and brain structure in unmedicated patients with bipolar and major depressive disorders. Brain Struct Funct 222:4051–4064.

He Z, Cui Q, Zheng J, et al. 2016. Frequency-specific alterations in functional connectivity in treatment-resistant and -sensitive major depressive disorder. J Psychiatr Res 82:30–39.

Hochberg Y, Tamhane AC. 1987. *Multiple Comparison Procedures*. Hoboken, NJ: John Wiley & Sons.

Iraji A, Miller R, Adali T, et al. 2020. Space: a missing piece of the Dynamic Puzzle. Trends Cogn Sci 24:135–149.

Jafri MJ, Pearlson GD, Stevens M, et al. 2008. A method for functional network connectivity among spatially independent resting-state components in schizophrenia. Neuroimage 39: 1666–1681.

Kaiser RH, Whitfield-Gabrieli S, Dillon DG, et al. 2016. Dynamic resting-state functional connectivity in major depression. Neuropsychopharmacology 41:1822–1830.

Kraus C, Kadriu B, Lanzenberger R, et al. 2019. Prognosis and improved outcomes in major depression: a review. Transl Psychiatry 9:127.

Li B, Liu L, Friston KJ, et al. 2013. A treatment-resistant default mode subnetwork in major depression. Biol Psychiatry 74:48–54.

Li J, Duan X, Cui Q, et al. 2019. More than just statics: temporal dynamics of intrinsic brain activity predicts the suicidal ideation in depressed patients. Psychol Med 49:852–860.

Li M, Zoltàn Z. 2017. The application of cluster analysis in ecnomics science. In: Proceedings of the 2016 2nd International Conference on Education, Social Science, Management

and Sports (ICESSMS 2016), Qingdao, China: Atlantis Press, 2017. www.atlantis-press.com/proceedings/icessms-16/25870756

Lin P, Yang Y, Gao J, et al. 2017. Dynamic default mode network across different brain states. Sci Rep 7:1–13.

Liston C, Chen AC, Zebley BD, et al. 2014. Default mode network mechanisms of transcranial magnetic stimulation in depression. Biol Psychiatry 76:517–526.

Lou HC, Luber B, Crupain M, et al. 2004. Parietal cortex and representation of the mental self. Proc Natl Acad Sci U S A 101:6827–6832.

Mayberg HS, Lozano AM, Voon V, et al. 2005. Deep brain stimulation for treatment-resistant depression. Neuron 45:651–660.

Monti RP, Lorenz R, Braga RM, et al. 2017. Real-time estimation of dynamic functional connectivity network. Hum Brain Mapp 38:202–220.

Otte C, Gold SM, Penninx BW, et al. 2016. Major depressive disorder. Nat Rev Dis Primers 2:1–21.

Pannekoek JN, Van Der Werff SJA, Meens PHF, et al. 2014. Aberrant resting-state functional connectivity in limbic and salience networks in treatment-naïve clinically depressed adolescents. J Child Psychol Psychiatry Allied Discip 55:1317–1327.

Perrone-Bertolotti M, Cerles M, Ramdeen KT, et al. 2016. The self-pleasantness judgment modulates the encoding performance and the default mode network activity. Front Hum Neurosci 10:1–12.

Posner J, Cha J, Wang Z, et al. 2016. Increased default mode network connectivity in individuals at high familial risk for depression. Neuropsychopharmacology 41:1759–1767.

Schiena G, Maggioni E, Pozzoli S, et al. 2020. Transcranial magnetic stimulation in major depressive disorder: response modulation and state dependency. J Affect Disord 266793–801.

Schwartz J, Ordaz SJ, Kircanski K, et al. 2019. Resting-state functional connectivity and inflexibility of daily emotions in major depression. J Affect Disord 249:26–34.

Sendi MSE, Zendehrouh E, Miller RL, et al. 2021. Alzheimer's disease projection from normal to mild dementia reflected in functional network connectivity: a longitudinal study. Front Neural Circ 14:593263.

Sharp R. 2015. The Hamilton Rating Scale for depression. Occup Med 65:340.

Sheline YI, Barch DM, Price JL, et al. 2009. The default mode network and self-referential processes in depression. Proc Natl Acad Sci U S A 106:1942–1947.

Silvanto J, Pascual-Leone A. 2008. State-dependency of transcranial magnetic stimulation. Brain Topogr 21:1–10.

Stevens FL, Hurley RA, Taber KH. 2011. Anterior cingulate cortex: unique role in cognition and emotion. J Neuropsychiatry Clin Neurosci 23:121–125.

Tibshirani R. 2011. Regression shrinkage and selection via the lasso: a retrospective. J R Stat Soc Series B Stat Methodol 73:273–282.

Tzourio-Mazoyer N, Landeau B, Papathanassiou D, et al. 2002. Automated anatomical labeling of activations in SPM using a macroscopic anatomical parcellation of the MNI MRI single-subject brain. Neuroimage 15:273–289.

Vergara VM, Mayer AR, Kiehl KA, et al. 2018. Dynamic functional network connectivity discriminates mild traumatic brain injury through machine learning. Neuroimage Clin 19:30–37.

Wainer J, Cawley G. 2021. Nested cross-validation when selecting classifiers is overzealous for most practical applications. Expert Systems with Applications, 182:115222. www.sciencedirect.com/science/article/abs/pii/S0957417421006540

Wang X, Öngür D, Auerbach RP, et al. 2016. Cognitive vulnerability to major depression: view from the intrinsic network and cross-network interactions. Harvard Rev Psychiatry 24:188–201.

Widge AS, Malone Jr DA, Dougherty DD. 2018. Closing the loop on deep brain stimulation for treatment-resistant depression. Front Neurosci 12:175.

Wise T, Marwood L, Perkins AM, et al. 2017. Instability of default mode network connectivity in major depression: a two-sample confirmation study. Transl Psychiatry 7:e1105.

Xiao X, Bentzley BS, Cole EJ, et al. 2019. Functional connectivity changes with rapid remission from severe major depressive disorder. bioRxiv. DOI: 10.1101/67215.

Yan CG, Chen X, Li L, et al. 2019. Reduced default mode network functional connectivity in patients with recurrent major depressive disorder. Proc Natl Acad Sci U S A 116:9078–9083.

Ye M, Yang T, Qing P, et al. 2015. Changes of functional brain networks in major depressive disorder: a graph theoretical analysis of resting-state fMRI. PLoS ONE 10:1–16.

Yu Q, Du Y, Chen J, et al. 2017. Comparing brain graphs in which nodes are regions of interest or independent components: a simulation study. J Neurosci Methods 291:61–68.

Zeng LL, Shen H, Liu L, et al. 2012. Identifying major depression using whole-brain functional connectivity: a multivariate pattern analysis. Brain 135:1498–1507.

Zhang S, Chen, JM, Kuang L, et al. 2016. Association between abnormal default mode network activity and suicidality in depressed adolescents. BMC Psychiatry 16:1–10.

Zhang Z, Liu G, Yao Z, et al. 2018. Changes in dynamics within and between resting-state subnetworks in juvenile myoclonic epilepsy occur at multiple frequency bands. Front Neurol 9:448.

Zhi D, Calhoun VD, Lv L, et al. 2018. Aberrant dynamic functional network connectivity and graph properties in major depressive disorder. Front Psychiatry 9:339.

Zhou Y, Yu C, Zheng H, et al. 2010. Increased neural resources recruitment in the intrinsic organization in major depression. J Affect Disord 121:220–230.

Zhu X, Wang X, Xiao J, et al. 2012. Evidence of a dissociation pattern in resting-state default mode network connectivity in first-episode, treatment-naive major depression patients. Biol Psychiatry 71:611–617.

Zou H, Hastie T. 2005. Regularization and variable selection via the elastic net. J R Stat Soc Series B Stat Methodol 67:301–320.

Address correspondence to:
Mohammad S.E. Sendi
Wallace H. Coulter Department of Biomedical Engineering
Georgia Institute of Technology and Emory University
Atlanta, GA
USA

E-mail: eslampanahsendi@gmail.com

Jing Sui
State Key Laboratory of Cognitive Neuroscience and Learning
Beijing Normal University
Beijing, China

E-mail: jsui@bnu.edu.cn

Vince D. Calhoun
Wallace H. Coulter Department of Biomedical Engineering
Georgia Institute of Technology and Emory University
Atlanta, GA
USA

E-mail: vcalhoun@gsu.edu